# FPMC2021-68277

## COMMUTATION LOSS IN HYDROSTATIC PUMPS AND MOTORS

## Robin Mommers, Peter Achten, Jasper Achten, and Jeroen Potma

Innas BV, Breda, The Netherlands E-mail: rmommers@innas.com, pachten@innas.com

#### **ABSTRACT**

In mobile hydraulic applications, more efficient machinery generally translates to smaller batteries or less diesel consumption, and smaller cooling solutions. A key part of such systems are hydrostatic pumps and motors. While these devices have been around for a long time, some of the causes of energy loss in pump and motors are still not properly defined. This paper focuses on one of the causes of energy loss in pumps and motors, by identifying the energy loss as a result of the process of commutation.

By nature, all hydrostatic pumps and motors have some form of commutation: the transition from the supply port to the discharge port of the machine (and vice versa). During commutation, the connection between the working chamber and the ports is temporarily closed. The chamber pressure changes by compression or decompression that is the result of the rotation of the working mechanism. Ideally, the connection to one of the ports is opened once the chamber pressure equals the port pressure. When the connection is opened too early or too late, energy is lost.

This paper describes a method to predict the commutation loss using a lumped parameter simulation model. To verify these predictions, experimental data of a floating cup pump was compared to the calculated values, which show a decent match. Furthermore, the results show that, depending on the operating conditions, up to 50% of all losses in this pump are caused by improper commutation.

#### **NOMENCLATURE**

Symb	Description	Unit
β	Swash angle	rad
$\epsilon$	Difference in efficiencies	-
$\eta$	Efficiency	-
ρ	Mass density	${ m kg}~{ m m}^{-3}$
$\phi$	Piston angle	rad
ω	Rotational speed	$\rm rad~s^{-1}$
$\boldsymbol{A}$	Surface area	$m^2$
C	Coefficient	-
K	Bulk modulus	Pa
m	Mass	kg
P	Power	W
p	Pressure	Pa
Q	Flow rate	${ m m}^{3}~{ m s}^{-1}$
R	Pitch radius	m
T	Torque	Nm
t	Time	S
V	Volume	$m^3$

# **Subscripts**

$\mathcal{C}$	Compression	loss	Loss term
com	Commutation	max	Maximum
d	Decompression	min	Minimum
H	High pressure port	p	Piston related
i	Piston index	q	Flow related
L	Low pressure port	rem	Remaining term

### 1 INTRODUCTION

In recent decades, the global energy consumption has been increasing exponentially. Between reducing the use of fossil fuels and the worldwide trend towards electrification, it has become essential to use as much of the available energy as possible. Therefore, energy efficiency is perhaps the most important issue of the current era. In order to design better, more efficient machinery, we need to understand how energy is lost.

To understand energy loss in electric motors for example, the total loss is typically split in up to six individual losses [1, 2]. Dividing total energy loss categorically like this, can help to determine which part of a system is responsible for which amount of loss. This in turn can help to design critical components in such a way that increases the energy efficiency of the machine.

In mobile hydraulic applications, more efficient machinery generally translates to smaller batteries or less diesel consumption, and smaller cooling solutions. A key part of such systems are the hydrostatic pumps and motors. It is currently still common practice to divide the loss of these machines into merely two categories: mechanical loss, and volumetric loss [3]. To really understand how to design better pumps and motors, a number of studies have focused on further dividing these losses into, for example, friction between moving components [4], dissipation in the lubrication gaps [5], and churning losses [6]. The current study focuses on another cause of energy loss in pumps and motors, by identifying the energy loss as a result of the process of commutation.

By nature, all hydrostatic pumps and motors have some form of commutation: the transition from the supply port to the discharge port of the machine (and vice versa). During commutation, the connection between the working chamber and the ports is temporarily closed. The chamber pressure changes by compression or decompression that is the result of the rotation of the working mechanism. Ideally, the connection to one of the ports is opened once the chamber pressure equals the port pressure. When the connection is opened too early or too late, energy is lost.

To determine how much energy loss is caused by this process of commutation, the next section will describe and analyse the operation of a simple, single piston, check-valve pump. An estimation of the commutation loss of this theoretical pump is

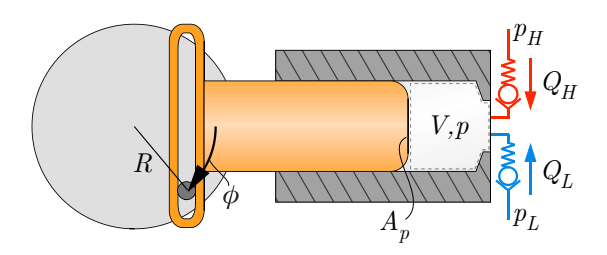


**Fig. 1**: Illustration of a simple, single piston check-valve pump.

made using a simulation model. Next, the proposed method is applied to the model of a floating cup type pump. The results of this model are compared to a set of experimental measurements using an actual 24 cc floating cup pump in different configurations. While the proposed method for determining the commutation loss is applied to a check-valve and a floating cup type pump, it can be applied to both pumps and motors of any type.

### 2 PUMP CYCLE

Figure 1 shows a simple, single piston, check-valve pump. The piston, shown in orange, has a cross sectional area  $A_p$ , and moves back and forth as a function of rotational angle  $\phi$  and the pitch radius R. The volume and pressure in the working chamber are shown as V and p, respectively. The working chamber is connected to both the low and the high pressure port ( $p_L$  and  $p_H$ ). Flow from these ports ( $Q_L$  and  $Q_H$ ) is defined as positive when oil flows into the chamber. For this pump, the chamber volume is described by:

$$V = V_{min} + RA_p \left[ 1 - \cos \left( \phi \right) \right] \tag{1}$$

## 2.1 (De)compression

At  $\phi=0$ , the piston is in its top dead center (TDC), and the chamber volume is at its minimum: the dead volume,  $V_{min}$ . Figure 2 shows the chamber volume, chamber pressure, and flow rate just after TDC, for two different discharge pressures. In the ideal situation, the chamber pressure in TDC is equal to  $p_H$ . As the angle increases, the chamber volume increases, resulting in a decreasing chamber pressure. During this period, both check valves are closed, so there is no flow in or out of the chamber. When the oil is expanded to a pressure level that is equal to pressure  $p_L$ , the check valve opens and oil flows into the working chamber. The chamber volume at that instance will be referred to as the decompressed volume  $V_d$ , at angle  $\phi_d$ .

$$V_d = V_{min} \frac{\rho_H}{\rho_L} \tag{2}$$

with  $\rho_L$  and  $\rho_H$  the mass density of the oil at pressure level  $p_L$  and  $p_H$ . The oil density and bulk modulus are derived using an isothermal oil model of Mobil medium DTE at 50°C [7]. This model was used for all of the results shown in this study.

As the chamber volume increases further, oil flows from the low pressure line into the chamber. At  $\phi=180^\circ$ , the piston arrives at the bottom dead center (BDC), and the chamber volume is at its maximum. Figure 3 shows the pump variables when the piston has past BDC. At this point in the pump cycle, the piston velocity switches sign, the connection to the low pressure port closes, and the chamber volume starts decreasing again. Since both valves are now closed, movement of the piston compresses the oil in the chamber volume to a higher pressure. When the pressure level

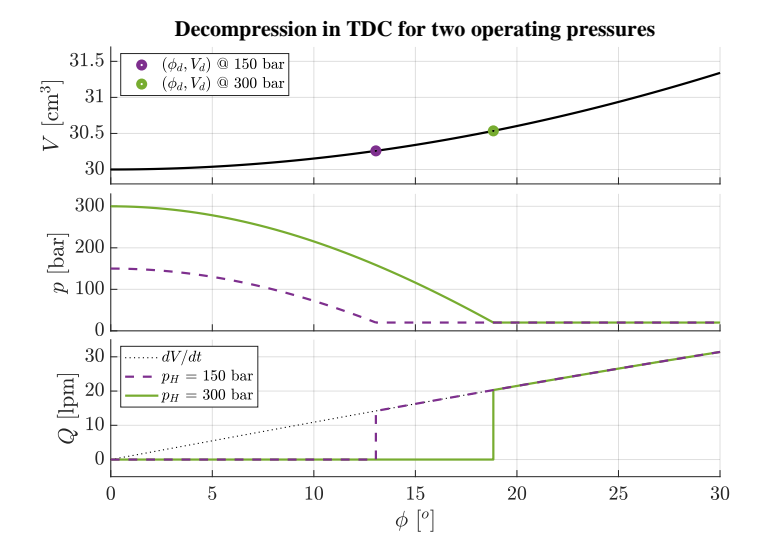


**Fig. 2**: Functions V, p, and Q in the working chamber in TDC during ideal cycle. Parameters:  $A_p = 5 \text{ cm}^2$ , R = 2 cm,  $V_{min} = 30 \text{ cm}^3$ ,  $p_L = 20 \text{ bar}$ ,  $\omega = 1000 \text{ rpm}$ .

equals  $p_H$ , the check valve opens and oil flows out of the working chamber into the high pressure port. The chamber volume at this instance will be referred to as the compressed volume  $V_c$ , at angle  $\phi_c$ .

$$V_c = (V_{min} + 2RA_p) \frac{\rho_L}{\rho_H} \tag{3}$$

#### 2.2 Flow rates

The total flow rate Q into the working chamber shown in fig. 2 and 3 is the sum of the two port flows.

$$Q = Q_L + Q_H \tag{4}$$

$$Q_x = C_q A_x \sqrt{\frac{2|p_x - p|}{\rho_x}} \cdot \operatorname{sign}(p_x - p), \qquad x = L \text{ or } H \quad (5)$$

In which  $C_q$  is the flow coefficient, and  $A_x$  is the cross sectional flow area of the connection between the working chamber and port x. Please note that a valve that is in the process of opening has a smaller flow area than the fully opened valve, as valves do not open instantaneous.

Looking at the ideal flow rates in fig. 2 and 3, we see that the flow rate is either zero, or the time derivative of the chamber volume.

$$Q_L = \begin{cases} 0 & \text{for } \phi < \phi_d \lor \phi \ge \pi \\ \dot{V} & \text{for } \phi_d \le \phi < \pi \end{cases}$$
 (6)

$$Q_H = \begin{cases} 0 & \text{for } \phi < \phi_c \\ \dot{V} & \text{for } \phi \ge \phi_c \end{cases} \tag{7}$$

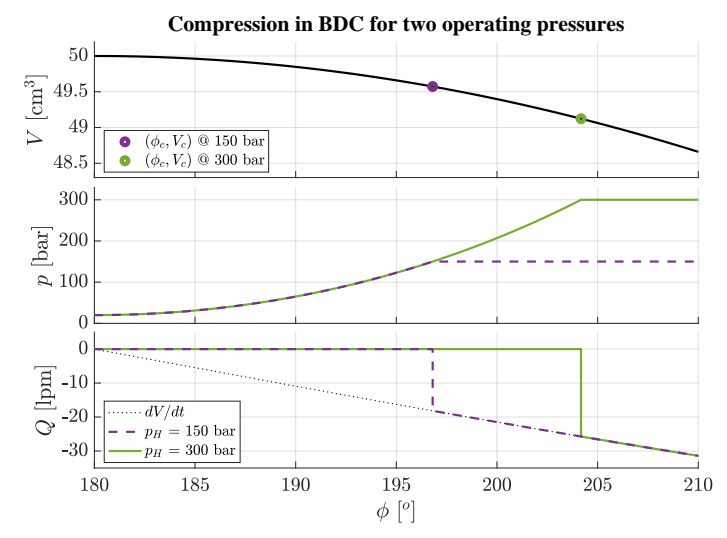


Fig. 3: Functions V, p, and Q in the working chamber in BDC during ideal cycle. Parameters:  $A_p = 5 \text{ cm}^2$ , R = 2 cm,  $V_{min} = 30 \text{ cm}^3$ ,  $p_L = 20 \text{ bar}$ ,  $\omega = 1000 \text{ rpm}$ .

The time derivative of the chamber volume is found to be:

$$\frac{dV}{dt} = \dot{V} = RA_p \omega \sin(\phi), \quad \text{with } \omega = \dot{\phi}$$
 (8)

with  $\omega$  the rotational speed of the axle.

## 2.3 Port flow loss

From eq. (5), it can be found that there is no flow without a pressure difference. With a large flow area  $A_x$ , this pressure difference can become very small, but never zero. Therefore, each flow has some power loss due to throttling. instantaneous throttling loss,  $\hat{P}_{thr}$ , in the example pump described above can be approximated by combining the throttle loss over both ports.

$$\hat{P}_{thr} = (p_L - p)Q_L + (p_H - p)Q_H \tag{9}$$

This means that even during the ideal pumping cycle, there are losses due to the throttling of the port flow rates. The size of this port flow loss can be estimated by finding the pressure in the working chamber. During the first half of the pump cycle, oil should flow from the low pressure port into the working chamber  $(p_L > p)$ . During the second part of the cycle, it is the other way around  $(p > p_H)$ . Combining eq. (5)-(8) results in the following relations for the pressure difference over the check valves.

$$p_{L} - p = \frac{\rho_{L}}{2} \left( \frac{\dot{V}}{C_{q} A_{L,max}} \right)^{2} \quad \text{for } \phi_{d} \leq \phi < \pi$$

$$p - p_{H} = \frac{\rho_{H}}{2} \left( \frac{\dot{V}}{C_{q} A_{H,max}} \right)^{2} \quad \text{for } \phi \geq \phi_{c}$$

$$(10)$$

$$p - p_H = \frac{\rho_H}{2} \left( \frac{\dot{V}}{C_q A_{H,max}} \right)^2 \qquad \text{for } \phi \ge \phi_c$$
 (11)

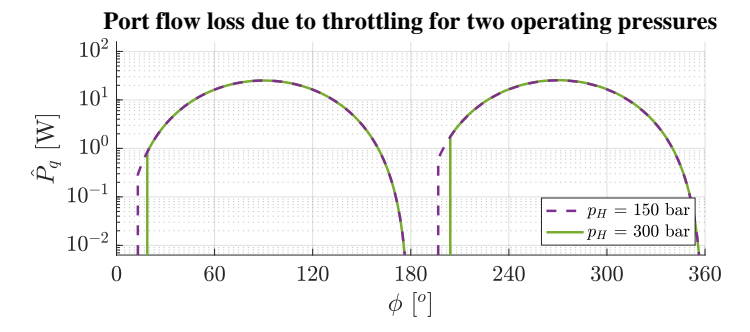


**Fig. 4**: Throttling loss during ideal cycle. Parameters:  $A_{L,max} = A_{H,max} = 2 \text{ cm}^2$ ,  $C_q = 0.7$ ,  $P_L = 20 \text{ bar}$ ,  $\omega = 1000 \text{ rpm}$ .

With  $A_{L,max}$  and  $A_{H,max}$  the maximum opening of the low and high pressure ports. We can combine these ideal pressure differences with the flow rates of eq. (6) and (7). Substitution in eq. (9) results in the port flow throttle loss,  $\hat{P}_q$ , in case of ideal commutation.

$$\hat{P}_{q} = \begin{cases} 0 & \text{for } \phi < \phi_{d} \\ \frac{\rho_{L}\dot{V}^{3}}{2C_{q}^{2}A_{L,max}^{2}} & \text{for } \phi_{d} \leq \phi < \pi \\ 0 & \text{for } \pi \leq \phi < \phi_{c} \\ -\frac{\rho_{H}\dot{V}^{3}}{2C_{q}^{2}A_{H,max}^{2}} & \text{for } \phi \geq \phi_{c} \end{cases}$$
(12)

Figure 4 shows these losses for the example pump shown before.

The average power loss due to port flow throttling can be determined by integration:

$$P_{q} = \frac{\omega}{2\pi} \int_{0}^{2\pi} \hat{P}_{q} d\phi$$

$$= \frac{\omega}{4\pi C_{q}^{2}} \left( \frac{\rho_{L}}{A_{L,max}^{2}} \int_{\phi_{d}}^{\pi} \dot{V}^{3} d\phi - \frac{\rho_{H}}{A_{H,max}^{2}} \int_{\phi_{c}}^{2\pi} \dot{V}^{3} d\phi \right)$$
(13)

## 2.4 Commutation loss

During each cycle, there are two periods in which there is no flow. In these periods, the working chamber is "commuting" from one pressure port to the other. All losses related to this commute are considered part of the commutation loss. In order for the described pump to have no commutation losses during the cycle, the opening and closing of the check-valves should happen instantaneous.

Figure 5 shows the results of a simulation of the described pump, with non-ideal check valves. In this figure, we see the chamber pressure, flow rate, and throttling losses around BDC. When the working chamber is commuting in BDC, the movement of the piston increases the pressure in the chamber. After the pressure  $p_H$  is reached, the check-valve starts to open. Since the valve is not yet fully open, oil flow out of the chamber is hindered. Chamber pressure increases to above the  $p_H$ , resulting in more

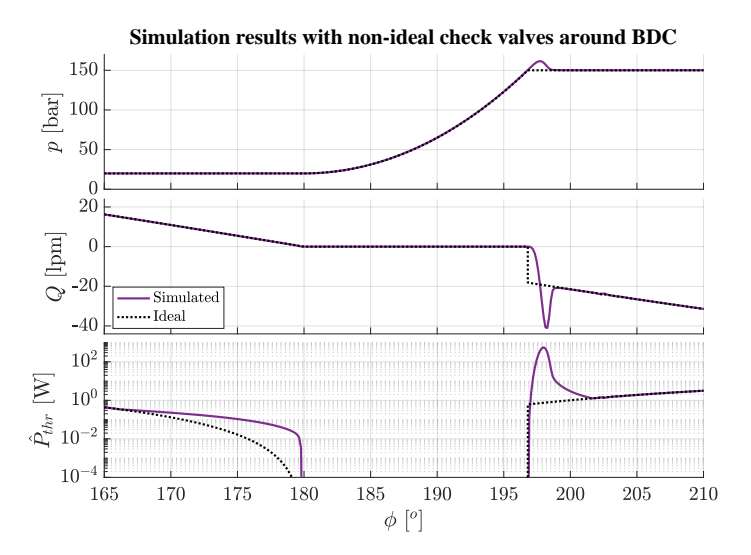


**Fig. 5**: Throttle losses around BDC following from a simulation model of the check-valve pump.

throttling losses. After the valve is fully open, the simulated flow rate follows the ideal flow rate.

From the numeric simulation, the throttling losses can be integrated. Since these losses contain both the port flow and the commutation loss, we find the commutation loss by subtracting the port flow losses:

$$P_{com} = \frac{\omega}{2\pi} \int_0^{2\pi} \left(\hat{P}_{thr}\right) d\phi - P_q \tag{14}$$

In which  $P_{com}$  is the average commutation loss; the product of the energy loss per rotation and the amount of rotations per second. The commutation loss can be calculated numerically, by integration of the throttle losses using simulation results. In the example shown, the chamber pressure and flow rate is very close to the ideal commutation. The commutation loss is calculated to be about 15 W, which is very close to ideal commutation as well. In theory, the described pump will have a power output of about 4.27 kW, which makes the commutation loss only 0.35% of the total power output.

## 3 FLOATING CUP SIMULATION MODEL

For check-valve pumps, like in the example shown above, the connection to the ports opens and closes based on pressure differences. Commutation is thus variable with respect to operating pressure. Other types of pumps often have a stationary commutation component (e.g. a valve plate). Unlike in a check-valve pump, such a pump will have additional commutation losses related to port timing. The following describes a simulation model of a pump type that uses a stationary commutation component: the floating cup pump.

## 3.1 Working chambers

In a floating cup pump, the working chambers (the cups) are separated from the barrel. Figure 6 shows a cross-sectional illustration of a working chamber with index i, with volume  $V_i$  and pressure  $p_i$ . The figure shows the pistons in orange, the cups in grey, and the barrel in green. The rotational angle  $\phi_i$  can be interpreted as the combination of barrel, cup, and piston moving to the right, while the piston makes a sinusoidal movement up and down. The flow from the high and low pressure port is defined by  $Q_{i,H}$  and  $Q_{i,L}$ , respectively.

The volume of the working chamber  $V_i$ , and its time derivative  $\dot{V}_i$  are described by:

$$V_i = V_{min} + RA_p \sin(\beta) \left(1 - \cos(\phi_i)\right) \tag{15}$$

$$\dot{V}_i = RA_p \sin(\beta) \omega \sin(\phi_i) \tag{16}$$

In which R is the pitch radius of the pistons,  $A_p$  the cross sectional area of the contact between the piston and cup,  $\beta$  the swash angle, and  $\omega$  the rotational speed of the pump. The derivative of the chamber pressure is given by:

$$\dot{p}_{i} = \frac{K(p_{i})}{V_{i}} \left( Q_{i,L} + Q_{i,H} - \dot{V}_{i} \right) \tag{17}$$

In which K is the bulk modulus (same isothermal oil model is used [7]), which is a function of the chamber pressure  $p_i$ .

### 3.2 Commutation unit

The amount of flow into and out of the working chambers is determined by two variable flow areas, which are illustrated as variable orifices in fig. 6. Since a floating cup pump uses a port plate for commutation, the size of these flow areas is a function of the piston angle  $\phi_i$ .

Figure 7 shows an illustration of a port plate, with the low pressure port in blue, and the high pressure port in red. The green shapes correspond to the openings in the bottom of the barrel, as shown in fig. 6. In the shown orientation, the barrel openings will rotate clockwise, starting at  $\phi = 0$  in the North of the figure. A magnification of port i (top right) shows that the connection to the low pressure port,  $A_{i,L}$  is only partly open. As the pump rotates, the connection will further open until a maximum is reached. A second magnification shows that the connection between barrel port i-1 and the high pressure port,  $A_{i-1,H}$ , is almost fully closed.

An example of the flow areas of the two ports as a function of the angle  $\phi_i$  is shown in fig. 8. This figure shows that the maximum opening of both ports is roughly 70 mm<sup>2</sup>. This flow area corresponds to the cross-sectional area of the green ports in the barrel. Furthermore, the two magnified parts of fig. 8 show the effect of the silencing grooves on the port openings. The flow rate over both ports is estimated using eq. (18) and (19).

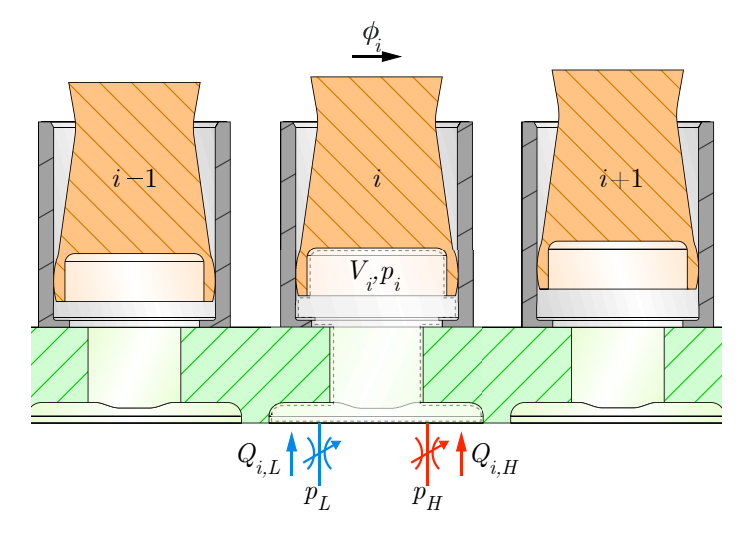


**Fig. 6**: Model parameters of piston-cup combination *i*. Piston in orange, cup in gray, barrel in green.

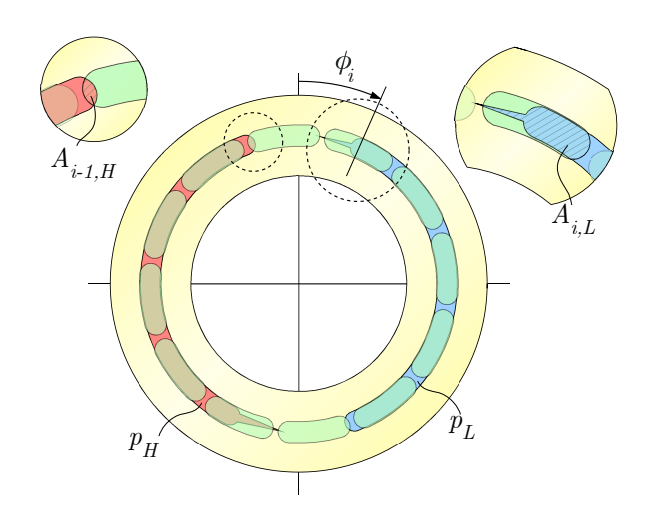
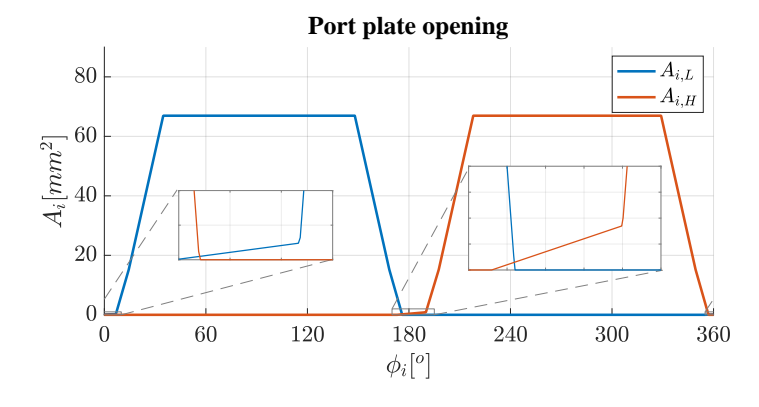


Fig. 7: Model parameters of port plate opening.



**Fig. 8**: Flow areas in the port plate as a function of  $\phi_i$ .

$$Q_{i,L} = C_q A_{i,L} \sqrt{\frac{2|p_L - p_i|}{\rho_L}} \cdot \operatorname{sign}(p_L - p_i)$$
(18)

$$Q_{i,H} = C_q A_{i,H} \sqrt{\frac{2|p_H - p_i|}{\rho_H}} \cdot \operatorname{sign}(p_H - p_i)$$
(19)

In which  $C_q$  is the flow coefficient, and  $\rho_L$  and  $\rho_H$  are the mass density of the oil at pressure levels  $p_L$  and  $p_H$ .

### 3.3 Commutation loss

In the example shown in fig. 8, we see that the connection to the high pressure port after BDC does not fully open until roughly 220°. As mentioned previously, the throttling losses that occur due to the ports not being fully open (or fully closed) are part of the commutation loss. Following the same logic as with the check-valve pump, the power loss due to throttling can be calculated for each working chamber, using eq. (20).

$$\hat{P}_{i,thr} = (p_L - p_i)Q_{i,L} + (p_H - p_i)Q_{i,H}$$
(20)

With  $\hat{P}_{i,thr}$  the instantaneous throttling loss of working chamber *i*. The flow loss and average flow loss in case of ideal commutation are very similar to eq. (12) and (13).

$$\hat{P}_{i,q} = \begin{cases} 0 & \text{for } \phi < \phi_d \\ \frac{\rho_L \dot{V}_i^3}{2C_q^2 A_{max}^2} & \text{for } \phi_d \le \phi < \pi \\ 0 & \text{for } \pi \le \phi < \phi_c \\ -\frac{\rho_H \dot{V}_i^3}{2C_q^2 A_{max}^2} & \text{for } \phi \ge \phi_c \end{cases}$$
(21)

$$P_{i,q} = \frac{\omega}{2\pi} \int_0^{2\pi} \hat{P}_{i,q} d\phi$$

$$= \frac{\omega}{4\pi C_q^2} \left( \frac{\rho_L}{A_{max}^2} \int_{\phi_d}^{\pi} \dot{V}_i^3 d\phi - \frac{\rho_H}{A_{max}^2} \int_{\phi_c}^{2\pi} \dot{V}_i^3 d\phi \right)$$
(22)

With  $A_{max}$  the maximum flow area for both  $A_{i,L}$  and  $A_{i,H}$ . Combining these with the relations found previously, we get the average commutation loss per piston,  $P_{i,com}$ .

$$P_{i,com} = \frac{\omega}{2\pi} \int_0^{2\pi} \left(\hat{P}_{i,thr}\right) d\phi - P_{i,q} \tag{23}$$

The total commutation loss is found by summing the commutation losses of the individual working chambers. Figure 9 shows an example of the resulting pressure, flow, and throttle loss of a single working chamber in a floating cup pump, around the BDC position. The simulated pump has 24 cups, and a total displacement volume of 23.7 cc per revolution. Looking at the flow rate  $Q_i$ , we see that there is already a flow (positive, so into the cup) before the BDC position is reached. This flow is coming from the high pressure port, as can be seen by the

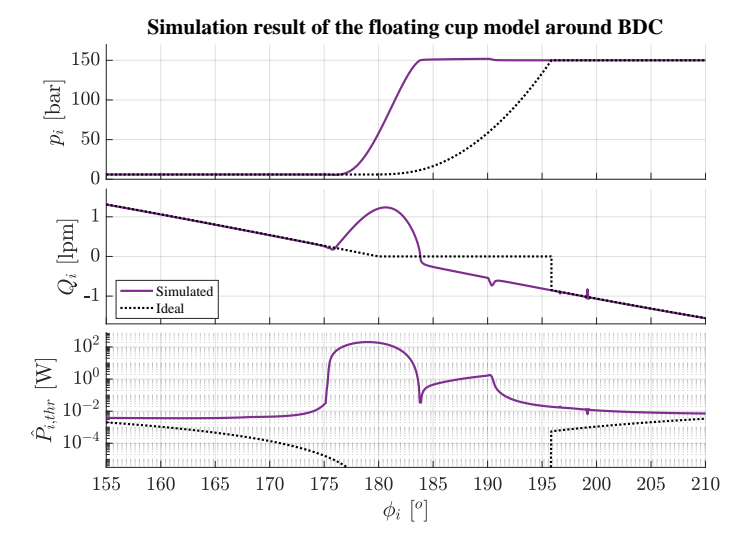


**Fig. 9**: Simulation results for a floating cup at  $p_H = 150$  bar,  $p_L = 6$  bar,  $\omega = 1000$  rpm.

increasing pressure  $p_i$ . In this case, the connection to the high pressure port seems to open too soon, resulting in a less than ideal commutation. Something similar happens in the TDC of this pump.

Using eq. (22) and (23), and the throttle loss shown in fig. 9, the total commutation loss of all cups is calculated to be roughly 87 W. In theory, this pump will have a power output of about 5.64 kW under these conditions, which makes the commutation loss 1.54% of the total power output.

## 3.4 Torque and flow loss

The proposed method for calculation of the commutation loss is based on determining the throttling loss of the flow into and out of the working chambers. While throttling is often linked to torque loss, commutation loss is not merely a torque loss.

In some hydrostatic machines, the commutation unit is designed such that the working chamber can be connected to both the high and low pressure port, mainly for the sake of noise-reduction [8]. In a pump, this means that some oil will flow back into the supply line, and will be missed at the discharge port. Traditionally, this part of the commutation loss would be called a volumetric loss, since flow is less than expected.

### 4 EXPERIMENTAL VALIDATION

As described above, the commutation loss is calculated using a simulation model. In order to validate these results, a floating cup pump has been tested using five different configurations, as shown in tab. 1. The difference between these configurations can be found in the combination of two components:

**Tab. 1**: Different configurations of the same floating cup pump.

#	Commutation unit	$V_{min}$ [cm <sup>3</sup> ]
1	Port plate 1: balanced	0.37
2	Port plate 2: optimal commutation	0.37
3	Port plate 3: four quadrant	0.37
4	Port plate 1: balanced	0.68
5	Port plate 1: balanced	0.97

#### Port plate design

Changing the dimensions of the commutation unit obviously has an effect on the timing of the ports opening, and therefore on the commutation loss. Three different options were tested:

- 1. Port plate with good commutation and low noise levels
- Port plate optimised to have lowest commutation loss (designed using the presented method for calculating commutation loss)
- 3. Port plate designed for operation in four quadrants
- Amount of dead volume  $(V_{min})$  per cup This has an effect on the amount of oil in the working chamber during commutation, and therefore on the decompression and compression angles  $(\phi_d \text{ and } \phi_c)$ .

## 4.1 Power loss and efficiencies

For each of the configurations, measurements were conducted at a wide range of operating conditions. The total power loss during these measurements was calculated using [9]:

$$P_{loss} = T\omega - \left[ p_H Q_H \left( 1 + \frac{p_H}{2\bar{K}} \right) - p_L Q_L \right]$$
 (24)

In which T is the measured torque, the indices L and H refer to the measured pressures and flow rates at the pump ports, and  $\bar{K}$  is

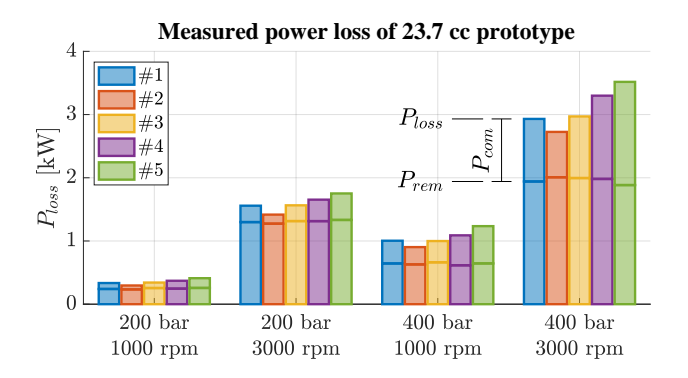


**Fig. 10**: Measured power loss for the five different configurations shown in tab. 1, at four operating conditions.

the average isentropic bulk modulus for the used oil (1.76e9 Pa). The overall efficiency,  $\eta$ , can be calculated as follows:

$$\eta = \frac{p_H Q_H \left(1 + \frac{p_H}{2K}\right) - p_L Q_L}{T\omega} = 1 - \frac{P_{loss}}{T\omega}$$
 (25)

The calculated power loss is split into two parts; the commutation loss,  $P_{com}$ , and the remaining loss,  $P_{rem}$ :

$$P_{loss} = P_{rem} + P_{com} \tag{26}$$

Figure 10 shows the measured power loss at four different operating conditions for each of the configurations (total height of the bars). Each of the results in fig. 10 additionally shows a line at the projected  $P_{rem}$ . It can be seen that the total loss is different between the different configurations. When the commutation loss for the specific configurations is subtracted, the projected  $P_{rem}$  seems to be relatively close between the different configurations.

Combining eqs. (25) and (26) results in:

$$\eta = 1 - \frac{P_{rem} + P_{com}}{T\omega} \tag{27}$$

The difference between the configurations is expected to only have an effect on the commutation loss. Therefore, the remaining loss  $P_{rem}$  will be more or less equal between the different configurations, as seen in fig. 10. To validate this statement, we can predict the efficiency that the pump would have if there were no commutation losses. This projected efficiency,  $\eta_{rem}$ , can be estimated using the commutation loss results from the simulation model

$$\eta_{rem} = 1 - \frac{P_{rem}}{T\omega} = 1 - \frac{P_{loss} - P_{com}}{T\omega}$$
 (28)

Figure 11 shows measurement results at 400 bar. The measured efficiency  $\eta$ , drawn with solid lines, shows that there is a clear difference between the different configurations. The difference between the best (#2) and the worst (#5) performing

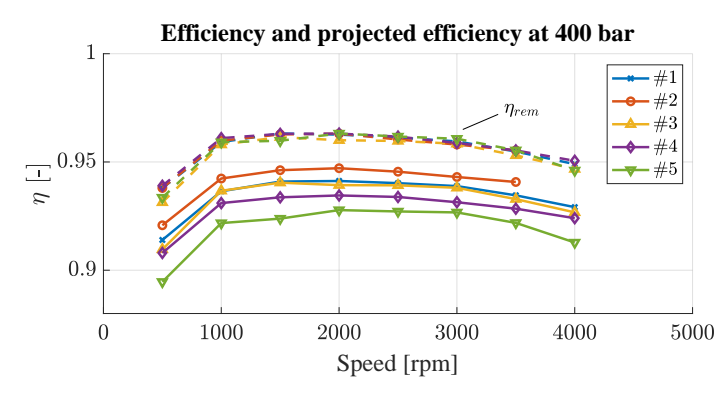


**Fig. 11**: Measured efficiency  $\eta$  (solid) and projected efficiency  $\eta_{rem}$  (dashed) of the different configurations at 400 bar.

configuration is roughly 2% over the full speed range. The dashed lines show the projected efficiency when the commutation loss is reduced to zero. The fact that these lines are all very close to each other, could indicate that the proposed method for estimating the commutation loss provides reasonable results.

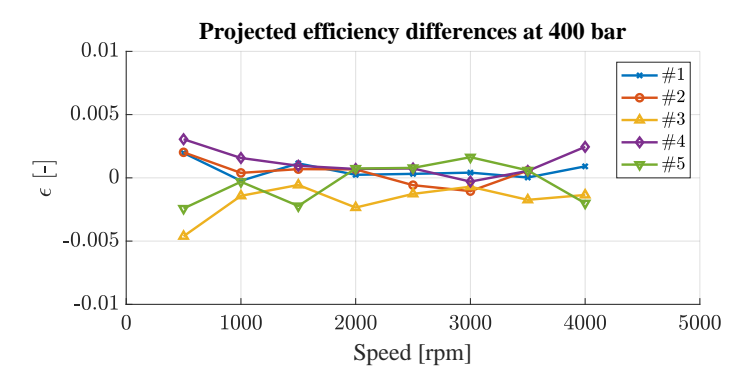
#### 4.2 Distribution of differences

For each operating point, the projected efficiency for configuration j,  $\eta_{j,rem}$ , can be compared to an average projected efficiency,  $\bar{\eta}_{rem}$ , at that operating point:

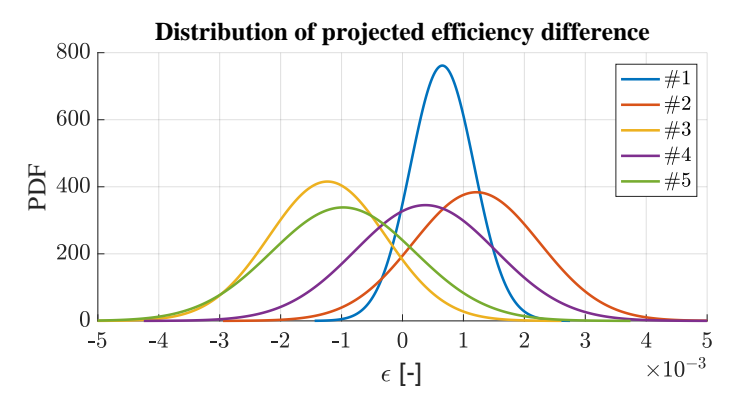
$$\varepsilon_j = \eta_{j,rem} - \bar{\eta}_{rem} \tag{29}$$

Figure 12 shows what this looks like for the results shown in fig. 11. In this figure, we see that at a speed of 500 rpm, the value of each  $\eta_{j,rem}$  is within 1% of the others ( $\pm 0.5\%$ ). At other speeds, the difference is smaller.

Calculation of the values of  $\varepsilon$  for a field of 32 operating points (100 to 400 bar, 500 to 4000 rpm) results in a distribution that is close to Gaussian. Figure 13 shows the probability density



**Fig. 12**: Difference between projected efficiency,  $\eta_{j,rem}$ , and average of projected efficiency,  $\bar{\eta}_{rem}$ , at each operating speed at 400 bar.



**Fig. 13**: Probability density functions of the  $\varepsilon$  values for all measured points in field of 32 measured operating conditions.

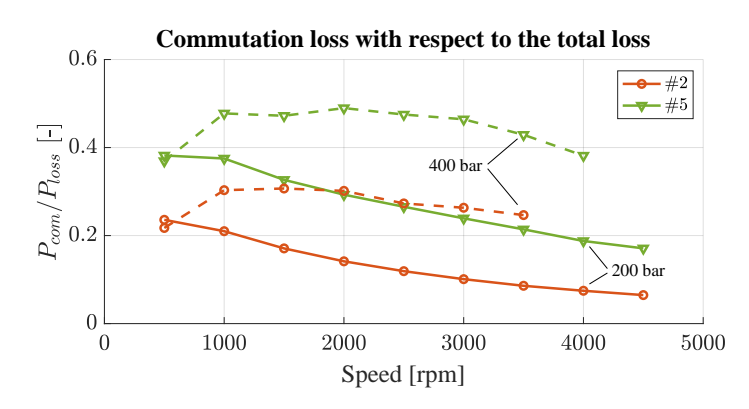
functions of these distributions for each of the configurations. If the model would estimate the commutation loss perfectly, all distributions would be centred around zero. In that case, the width of the density function would be caused by measurement inaccuracies alone.

Figure 13 shows that there are some trends in the values of  $\varepsilon$ . For example, the projected efficiency of configurations 3 and 5 are slightly lower than the rest for most of the time (PDF mostly negative). Overall it can be found that the values of the projected efficiency per operating condition are on average within 0.25% of each other ( $\pm 0.125\%$ ). This suggests that the calculation of the commutation loss could be a reasonable indication of the commutation loss in a pump.

## 5 IMPACT OF COMMUTATION LOSS

Comparing the measurement results of the tested configurations to the calculated commutation loss provides an insight in the impact of the commutation loss on the total performance of the pump. From the presented configurations in tab. 1, configuration 2 has the lowest commutation loss, while configuration 5 has the largest. Figure 14 shows the size of the commutation loss with respect to the total power loss that was measured, for these two configurations.

Figure 14 shows that at a discharge pressure of 200 bar, the relative size of the commutation loss decreases as the rotational speed increases. At 4500 rpm, the commutation loss is found to be 6.6% of all losses for configuration 2, and 17.5% for configuration 5. At a larger discharge pressure of 400 bar, the commutation loss of configuration 5 is expected to be almost half (49.4%) of all losses at 2000 rpm. From these results, it is found that the design of the commutation unit in combination with the dead volume has a significant effect on the commutation loss. Moreover, this effect is predictable, and can be used to optimize these components such that commutation loss is minimal.



**Fig. 14**: Commutation loss compared to the total loss, of two configurations, at two pressure levels.

Even though configuration 2 was designed to have minimal commutation losses, there is still a significant part of the power loss that is caused by a non-ideal transition between the two ports. As shown in fig. 14, the commutation loss is found to be responsible for 20 to 30% of all power loss at 400 bar, for the presented floating cup pump. As mentioned in the introduction, understanding losses and being able to predict these losses helps to design better pumps. Now that a model for calculating the commutation losses is introduced, a promising technology was developed that has the potential to reduce the commutation losses to a negligible level. This so-called 'shuttle' technology was first introduced for use in hydraulic transformers in 2001 [10], but has recently been further developed for use in pumps and motors as well [11].

### 6 CONCLUSION

In order to improve the performance of hydrostatic pumps and motors, we need to understand what causes power loss in such machines. One of these causes is the power loss that occurs as a result of the process of commutation. This study presents a method to calculate the commutation loss. The simulated losses of five different floating cup pumps were compared to the outcome of real life measurements. There is a decent match between the predicted loss and the measured loss. This seems to indicate that the proposed method can provide a useful tool in the process of designing pumps and motors such that the commutation loss is minimal.

## **REFERENCES**

- [1] IEEE standard test procedure for polyphase induction motors and generators. *IEEE Standard 112-B*, 2004.
- [2] IEC 60034-2-1:2014 rotating electrical machines-part 2 1: Standard methods for determining losses and efficiency from tests (excluding machines for traction vehicles). 2014.
- [3] ISO4409:2019. Hydraulic fluid power, positive displacement pumps, motors and integral transmissions; Methods of testing and presenting basic steady state performance. International Organization for Standardization, 2019.
- [4] Hong, Y.-S. and Doh, Y.-H. Analysis on the friction losses of a bent-axis type hydraulic piston pump. *KSME international journal*, 18(9):1668, 2004.
- [5] Ivantysynova, M. and Baker, J. Power loss in the lubricating gap between cylinder block and valve plate of swash plate type axial piston machines. *International Journal of Fluid Power*, 10(2):29–43, 2009.
- [6] Zhang, J., Li, Y., Xu, B., Pan, M., and Lv, F. Experimental study on the influence of the rotating cylinder block and

- pistons on churning losses in axial piston pumps. *Energies*, 10(5):662, 2017.
- [7] Witt, K. Die berechnung physikalischer und thermodynamischer kennwerte von druckflüssigkeiten, sowie die bestimmung des gesamtwirkungsgrades an pumpen unter berücksichtigung der thermodynamik für die druckflüssigkeit. 1974.
- [8] Seeniraj, G. K. and Ivantysynova, M. Multi-objective optimization tool for noise reduction in axial piston machines. SAE International Journal of Commercial Vehicles, 1(2008-01-2723):544–552, 2008.
- [9] Achten, P., Mommers, R., Nishiumi, T., Murrenhoff, H., Sepehri, N., Stelson, K., Palmberg, J.-O., and Schmitz, K. Measuring the losses of hydrostatic pumps and motors; a critcal review of iso4409:2007. In *BATH/ASME 2019 Symposium on Fluid Power and Motion Control*. American Society of Mechanical Engineers, 2019.
- [10] Achten, P., Vael, G., van den Oever, J., and Fu, Z. 'Shuttle' technology for noise reduction and efficiency improvement of hydrostatic machines. In *The Seventh Scandinavian International Conference on Fluid Power*, page 269, 2001.
- [11] Mommers, R. and Achten, P. 'Shuttle' technology for noise reduction and efficiency improvement of hydrostatic machines - part 2. In BATH/ASME 2021 Symposium on Fluid Power and Motion Control. American Society of Mechanical Engineers, 2021.